Chapter 5

Structural and Phase Transition Classification

Knowing the order of the structural phase transitions of Ag_2Se, Cu_2Se, and $Cu_{1.97}Ag_{0.03}Se$ is essential to understanding their thermoelectric properties in the vicinity of those phase transitions. Structure effects the transport properties through the mechanism of the electronic band structure and the phononic band structure. A change in band structure should always be accompanied by some, though perhaps subtle, change in structure. In later chapters I will present the transport properties of Ag_2Se, Cu_2Se, and $Cu_{1.97}Ag_{0.03}Se$, and there will be direct correlations between the structural changes of their phase transitions in their transport property. Understanding the nature of that transformation will allow me to develop the phenomenology necessary to explain them.

In the case of Cu_2Se there is an important scientific question that was answered by the work presented here. All previous authors considered Cu_2Se to be a first order phase transition [21, 41, 188, 191, 123, 121]. The work presented here shows it to be definitively second order [23]. This question of is central importance; the zT of Cu_2Se can not be properly calculated without understanding the nature of its phase transition. The determination of the Differential Scanning Calorimetry (DSC) data depends on the order of the phase transition. A substantial broad peak is seen in the DSC for Cu_2Se, see Figure 5.1. If the transition is second order the DSC measurement must be treated as c_p. If it were first order, it would be more proper to

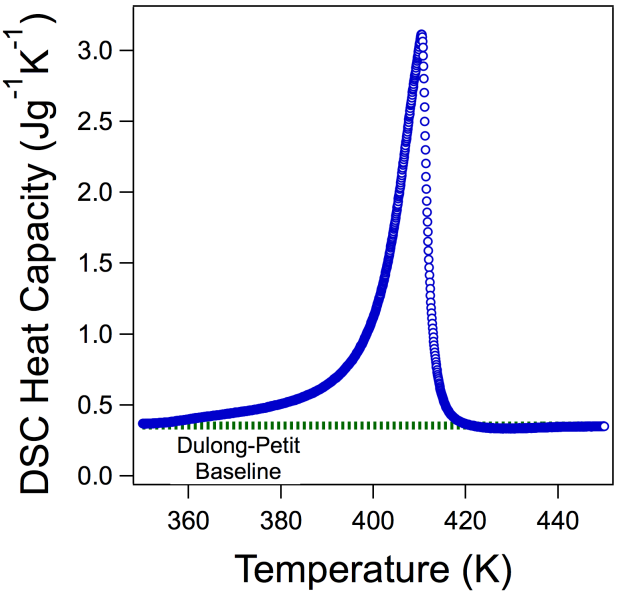

Figure 5.1: Differential Scanning Calorimetry c_p for Cu_2Se (blue circles) with the Dulong-Petit contribution as a green dotted line. Determining the order of the phase transition of Cu_2Se determines which of these two curves should be used to calculate c_p.

use the Dulong-Petit heat capacity instead.

As κ is calculated from c_p by the formula $\kappa = \rho c_p D_t$, and zT from κ by $zT = \alpha^2 \sigma T/\kappa$, this argument has an order of magnitude impact on the zT calculated. Treating Cu_2Se as a first order transition results in a five-fold overestimate in zT above its true value. Answering this question is particularly pressing due to recent published articles, [121, 123], claiming zTs two to five times that published here based on a first order treatment of c_p data.

Ag_2Se has a much simpler story. Prior literature shows understanding of its transformation as first order [15, 137, 21]. The work presented below agrees with that assessment. Still, it serves an excellent contrast to Cu_2Se and therefore illuminates the contrast between first and second order behavior in structural measurements.

$Cu_{1.97}Ag_{0.03}Se$ has the most complex story and one that this thesis does not fully resolve. As temperature is increased from room temperature it follows a trend similar to than of its Cu_2Se main phase. However, this trend is interrupted by the dissolution of a secondary phase of CuAgSe, eventually leading to a first order phase transition

at a temperature lower than Cu_2Se's second order phase transition.

In the next section I will discuss the definitions, different categorizations of, and phenomenology of structural phase transitions. There will be particular emphasis on order-disorder phase transitions. In section 5.2 I will discuss the measurements made on Ag_2Se, in section 5.3 I will discuss the characterization made of Cu_2Se, and in section 5.4 I will discuss measurements made on $Cu_{1.97}Ag_{0.03}Se$.

From understanding of the structure of a material, great insight can be obtained into its chemical performance can be obtained. For example, if the structure is well-understood, calculations of the electron and phonon band structure can be accomplished by Density Functional Theory (DFT). Super-ionic materials are a particularly challenging and interesting topic for structural studies. The high mobility and interstitial occupation probabilites of their ions means that determining the average location of the ions is insufficient for understanding their transport. For this work I am of course interested primarily in the nature of the superionic phase transition of Cu_2Se, Ag_2Se, and related materials.

5.1 Phase Transitions

A phase transition is a transformation in the symmetry of a system. The symmetries are understood in terms of the mean location or state of the degree of the system (*e.g.*, atoms, molecules, spin states). For example, the Arrhenius activation of Frenkel ion defects does not affect the mean symmetries and so is not a phase transition. Phase transitions are a very broad category. In a glass transition the symmetry reduction is purely local [162]. In crystal twinning or martensite transitions the reduction in order is between large ordered grains rather than due to a local effect [162]. In order-disorder transitions a local change in coordination results in a long-range transformation in symmetry [95]. An excellent summary of phase transitions in the solid state is available in Rao and Rao [162]. Super-ionic phase transitions are *order-disorder* phase transitions [21, 151].

The disordering is frequently modeled as due to the creation of Frenkel defects [163,

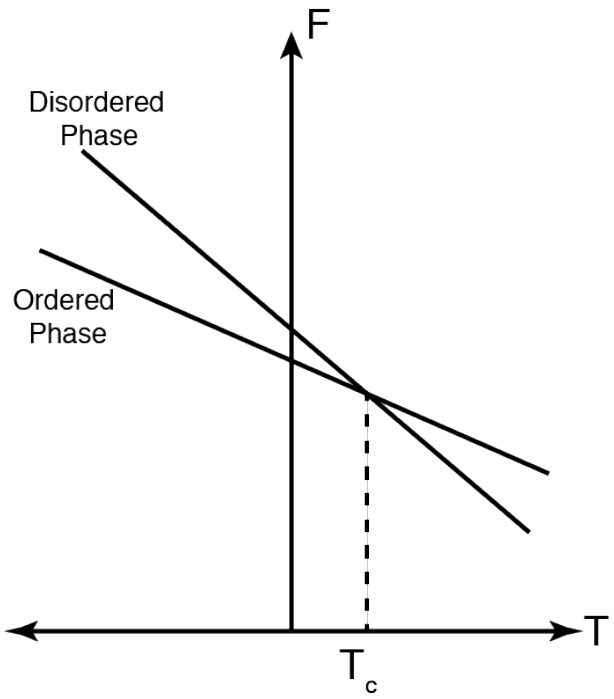

Figure 5.2: Free energy versus temperature for a first order phase transition. At T_c the free energy of both phases is equal.

22, 70, 34] in the high temperature phase; while this may be true for other super-ionics, the pair distribution function (PDF) data measured for my publication on Cu_2Se [23] contradicts this explanation. Super-ionics typically have an ionicity close to the critical value of 0.785 [22] described by Phillips [156]. Therefore there is almost equal preference for coordination into sites preferred by ionic coordination as those preferred by electronic coordination. Aniya [4, 5] suggested that it is the fluctuations between these two co-ordinations that are characteristic of superionic materials; this explanation is more compatible with our PDF data.

In an order-disorder phase transition all high-temperature symmetries are preserved in the low temperature phase. Solidification of a liquid, in which the rotational freedom of the liquid is lost but the chemical coordination maintained, is a very common instance of an order-disorder transition [31]. In an order-disorder transition the ordering is typically long range, mathematically defined as a very slow decay of correlations between states of the ordering element with increasing distance. The kinetics of an order-disorder transition are relatively fast, as they are not limited by atomic

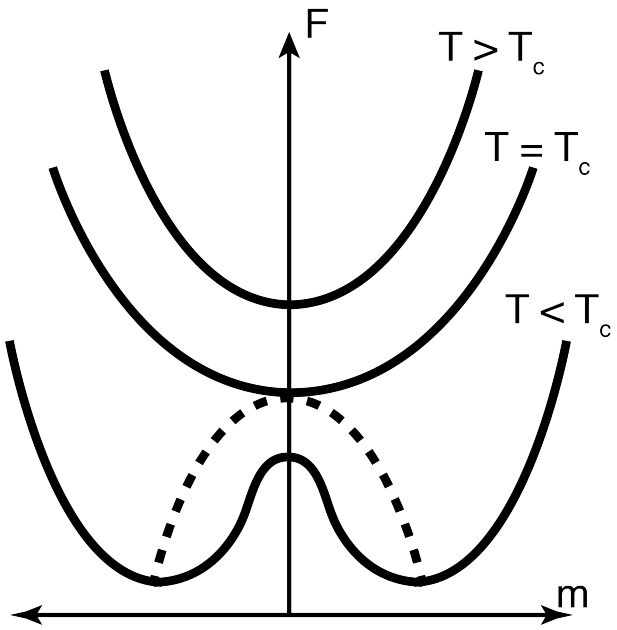

Figure 5.3: Free energy (F) versus order parameter (m) for a second order transition. Each of the curves is on its separate axis. The dotted line represents the equilibrium order parameter. As T goes to T_c, m goes continuously to zero.

diffusion.

5.1.1 Order-Disorder Phase Transitions Type

There are two principle types of order-disorder phase transitions. First order transitions are characterized by a first derivative discontinuity in a thermodynamic state parameter. This is typically measured by the instantaneous change in the volume or enthalpy as a thermodynamic parameter is changed [162]. A second order transition shows a discontinuity in a second or higher order derivative of the thermodynamic quantities. Certain second order transitions, including that of Cu_2Se, have a derivative of free energy that diverges to infinity at the phase transition temperature. Under the old classification system of Ehrenfest these were not considered second order transitions [53]. Instead they were called λ-transitions for the characteristic λ-shape in the dependence of their heat capacity on temperature [65, 157]. In more modern classification systems based on the work of Landau and Ginzburg, all phase transitions with continuous transformation of free energy are considered to be second order or

continuous [95].

Thermodynamic stability must be determined by a formulation that includes it. This formulation is the Free Energy. Without loss of generality, I use the Helmholtz Free (F) energy rather than Gibbs Free Energy. The difference between these two formulations is whether the system is held at constant volume (Helmholtz) or constant pressure (Gibbs); that detail is irrelevant to the argument below. For any given phase, defined as a set of symmetries obeyed by its degrees of freedom, the free energy is:

$$F_i = U_i - TS_i \tag{5.1}$$

There are as many phases as one can dream up. Very few are thermodynamically favorable. At a given set of thermodynamic conditions (*e.g.*, P,T) there will be only one phase or set of phases stable at a temperature. This phase or combination of phases is that which has minimal F_i. Each of these different phases will have a different U_i and S_i. A phase with higher entropy and high internal energy (*i.e.*, a gas) will be more stable at high temperatures than phase with low internal energy and low entropy (*i.e.*, a liquid); the converse is also true. If U_i and S_i are known for both phases the temperature of transition me determined by setting Equation 5.1 equal for each phase. Defining $\Delta U = U_i - U_j$ and $\Delta S = S_i - S_j$, this is equivalent to:

$$\Delta U = T\Delta S \tag{5.2}$$

As a very simple example consider the dissociation of diatomic oxygen into monatomic oxygen. In this hypothetical example $\Delta S = R/2$ where R is the gas constant while $\Delta U = 495 kJ/mol$. Therefore the temperature of the phase transition is ≈60,000 K — and indeed monatomic oxygen is very rarely observed.

In the case of the super-ionic transition ΔU is the energy that prefers the ions to be ordered in some way — perhaps a bond energy or the effect of alignment of a dipole with the crystal field — while ΔS is the additional configurational entropy available to the disordered phase. This may not be straightforward to calculate, as a substantial portion of the lifetime of super-ionics is spent between lattice sites in

regions of non-minimal potential [87]. Still, a simple configurational entropy argument helps to contextualize the scale of the phase transition. Following Korzhuev [103], if we assume that there are n_0 accessible vacancies per mobile ion in the super-ionic state then ΔS should be:

$$\Delta S = R \ln(n_0) \tag{5.3}$$

For $n_0 = 3$, $\Delta S = 9.1\,\mathrm{J \cdot mol^{-1}K^{-1}}$. This is comparable to the entropy of melting.

If ΔS and ΔU are themselves independent of temperature, than there will be a first order phase transition. The difference in the free energy between the two states decreases until the high entropy state becomes more favorable at $T = T_c$. (Figure 5.2). Because the high entropy phase requires input of heat equal to $T\Delta S$ in order to form, there is frequently hysteresis in measurments through first order phase transitions. On heating the temperature rises above T_c, but the material remains ordered until sufficient heat has been absorbed to complete the phase transition. On cooling at a steady rate, a similar but opposite effect occurs. Measurements on heating overestimate the phase transition temperature while measurements on cooling underestimate it.

The assumption that ΔU and ΔS are constant as a function of temperature is generally invalid. Disordering can occur without a phase transition at all. For a phase transition to occur there must be a fundamental change in the symmetry of a system. For example, Arrhenius activation of defects will increase the internal energy and entropy slightly. This will increase T_c slightly and decrease the enthalpy of formation of the transition, but it will not eliminate it. That entropy increase is still much smaller than the entropy increase of the disordering phase transition. It will change the slopes and perhaps add curvature to the lines in Figure 5.2, but the lines will still intercept at an angle. That angle represents the entropy of the transition.

In order for the transition to be continuous rather than abrupt the two curves in Figure 5.2 must intercept tangent to one another, as thermodynamics requires the free energy by analytic for any given phase [31]. Therefore a continuous transition requires that the entropy of the ordered phase increases continuously and that its

internal energy increases continuously to the phase transition temperature. This requires the disordering process to be continuous rather than abrupt.

In proximity to an order-disorder phase transition the free energy is described in terms of an order parameter. For example, in the canonical case of a spin-ordering transition the order parameter is the average spin magnetization. The super-ionic order parameter is theorized to relate to the relative population of different sites by the mobile ion [151, 70]. The free energy contribution associated with the ordering — which is the only free energy terms that differentiates the ordered and disordered phase — is for a first order transition:

$$F = am^2 + bm^4 + cm^3 \tag{5.4}$$

The cubic term leads to a discontinuity in the value of m at $T = T_c$.

For a second order transition the Landau Free Energy is:

$$F = am^2 + bm^4 \tag{5.5}$$

As the phase transition is approached thermodynamic quantities follow critical power laws. For example, the order parameter decreases to zero continuously:

$$m = m_0 \left(\frac{T_c - T}{T_c} \right)^{\beta} \tag{5.6}$$

In which β is called the critical exponent. Order parameter in a structural transformation is related to the diffractogram peaks, so a related power law should be discoverable by analyzing those peaks. A similar power law is expected for heat capacity.

Another type of phase transition is a co-existence phase transformation. This is a temperature extended first order phase transtion. some interaction (*i.e.*, pressure) between the concentration of the two phases elongates the region over which the low-temperature phase transforms into the high temperature phase. This sort of phase is easily distinguished from a true second order transition by diffractogram. In a

coexistence transition the intensities will vary as one phase steadily appears and the other steadily disappears, but the angles at which they have diffraction peaks will remain steady.

A final type of phase transition is a *weakly first-order* phase transition [16]. In this type the symmetry between the multiple minima in free energy is weakly broken so that the two minima in Figure 5.3 are slightly displaced from one another. At temperatures well below the phase transition temperature the symmetry breaking appears very similar to a second order transition, except that one minima is global and so slightly preferred. At temperature near the phase transition this tiny offset is large compared to the difference between the ordered state's minimum and the disordered states minimum, and a first-order aspect of the transition appears. Whenever a lambda type second order transition is heated or cooled through its phase transition at a finite rate, it is to some degree weakly first order. The heat capacity at T_c is infinite and so for even a very slow heating rate and very good connection of the sample to a thermal bath, there will be a moment at which the correct heat cannot be supplied.

5.2 Ag_2Se

The high temperature structure and phase transition of Ag_2Se were first noted by Rahlfs in 1934 [161]. In the high temperature structure ($Im3\bar{m}$) the selenium is body-centered cubic, while silver ions occupy the interstitial sites. The more complex low temperature phase was described by Wiegers [198]. The silver sits on two sites in the low temperature phase. One of the silver sites is coordinated tetrahedrally by four selenium atoms and the other is coordinated trigonally planar to three selenium atoms.

A diffractogram was measured at room temperature from $2\theta = 10^\circ$ to $2\theta = 100^\circ$. The sample was then heated at 1K per minute to 450 K (well above the nominal phase transition temperature of 413 K [136]. A diffractogram was measured at that temperature as well. The sample was cooled at 1K per minute to room temperature and

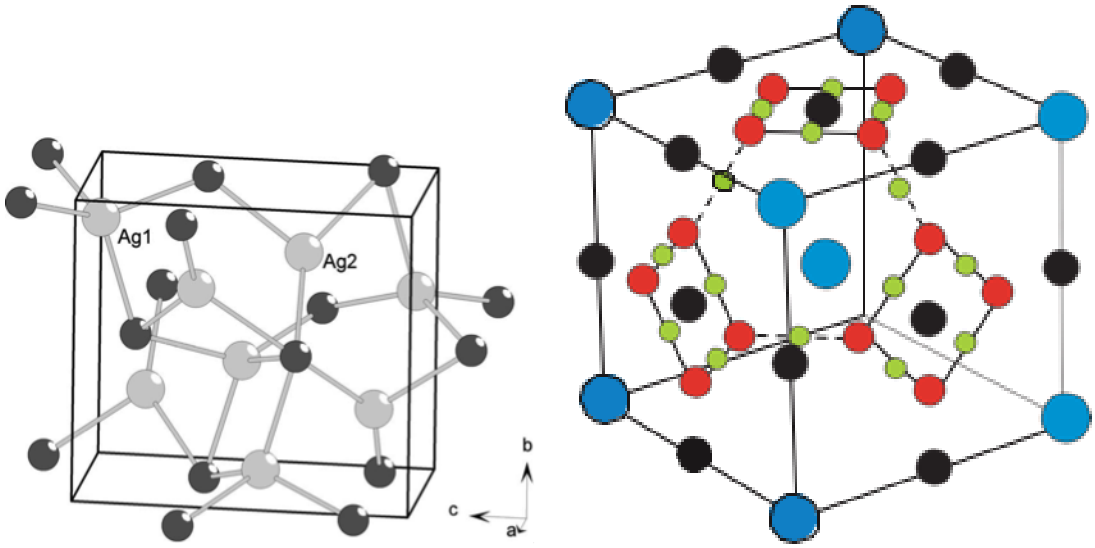

Figure 5.4: Low Temperature (a) [15] and high temperature (b) [18] structure of Ag_2Se

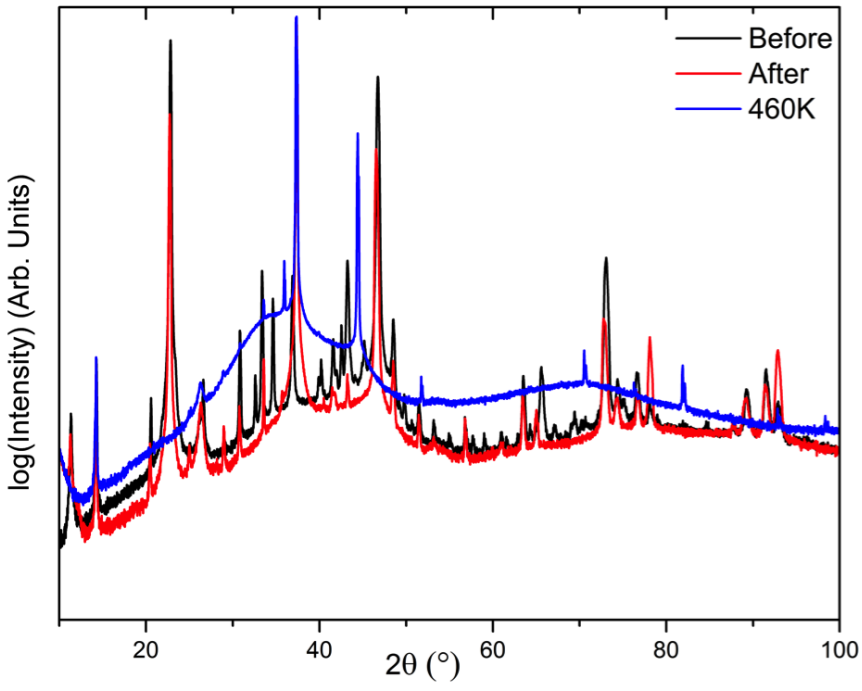

Figure 5.5: Powder X-Ray Diffractogram for Ag_2Se above and below its phase transition. All symmetries of the high temperature phase are present in the low temperature phase.

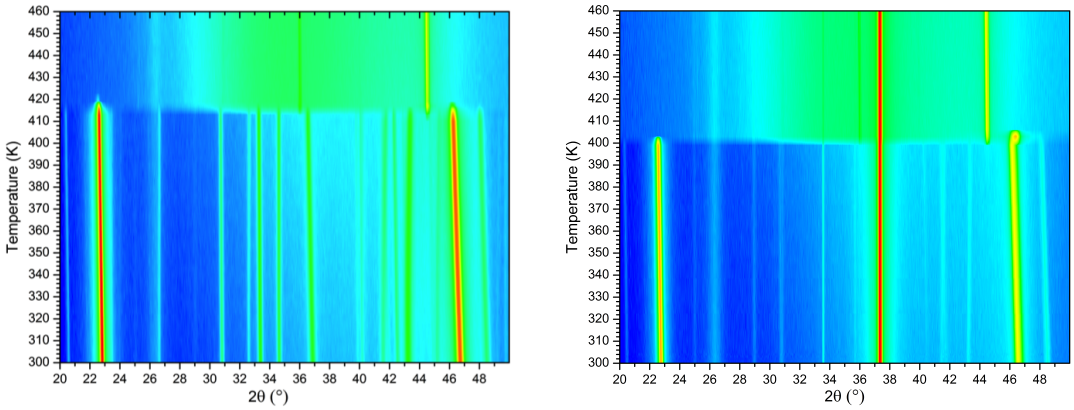

Figure 5.6: Temperature dependent X-ray diffractograms measured on heating (a) and on cooling (b) of Ag_2Se. A first order transition is seen at 415 K on heating and 401 K on cooling.

a third diffractrogram measured. All three diffractograms are shown in Figure 5.5(a).

Both above [145] and below [207] the transition the measured peaks index to previously published data, however large intensity mismatches are observed. These intensity mismatches were also observed by Billeter *et al.* [15] and ascribed to Se precipitation. This problem is likely more significant in the powder XRD as compared to bulk samples due to their larger surface area to volume ratio. No Ag is visible in the diffraction patterns at any temperature. Since a bulk synthesis product was used, large grain sizes are expected and the observed intensity mismatch is ascribed to this. The low temperature modification is orthorhombic (Space group $P2_12_12_1$) which explains the different dependences of the peak positions below the transition. The low temperature space group maps homomorphically to the high temperature space group ($Im\bar{3}m$); that is, all symmetries of the low temperature phase are preserved in the high temperature phase.

During the heating and cooling process diffractograms were measured from $2\theta = 20°$ to $2\theta = 52°$ in order to determine the nature of the phase transition. The duration of each scan was three minutes and consequently the temperature changed by 3 K from start to end of each scan. From inspection of a color map of this data there is a first order phase transition observed at 415 K on heating (Figure 5.6(a)) and 401 K on cooling (Figure 5.6(a)), with the phase transition temperature halfway in between

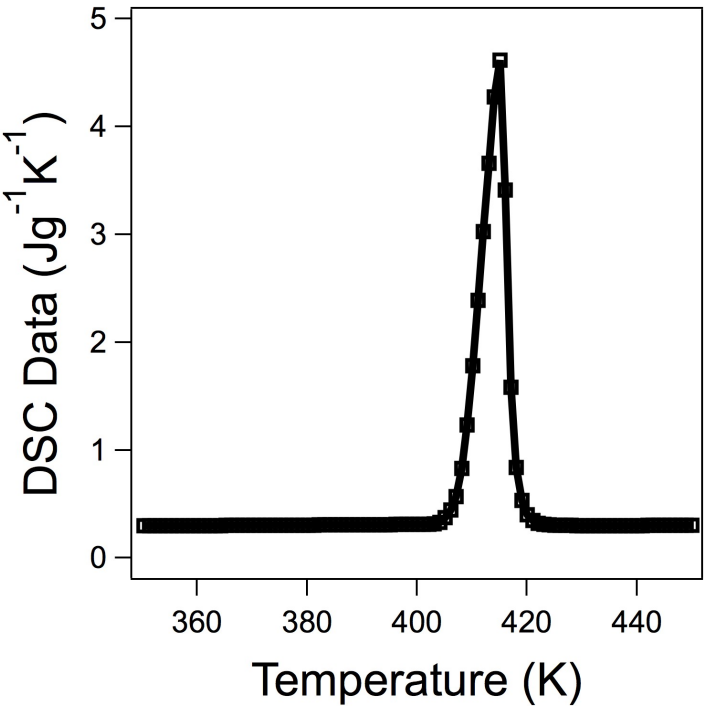

Figure 5.7: Differential Scanning Calorimetry data for Ag_2Se

at $T_c = 408$K. This is consistent with literature reports [15, 136]. The discrepancy of the phase transition on heating and cooling is characteristic of a first order process and a consequence of the non-adiabatic heating.

The color maps show strongly diffuse background scattering. While significant in the low temperature phase, in the high temperature phase it makes distinguishing the peaks visually almost impossible. This suggests diffuse scattering, much like in a glass, that may cause phonon scattering and low thermal conductivity. The exception is a sharp peak at $2\theta = 37.2°$ that is visible on cooling but not on heating.

Differential scanning calorimetry data for Ag_2Se(Figure 5.7(a)) shows a sharp symmetric peak centered at 414 K. This peak is characteristic of a first order transition. Due to the preponderance of literature [15, 137, 21] evidence and the crystallographic evidence presented above for Ag_2Se's first order transition, it was unnecessary to confirm the order of the phase transition via altering the heating rate. The region of elevated calorimetry data extends from 402 K to 426 K. The DSC curve of a first order transition should *begin* to increase at the phase transition temperature. By

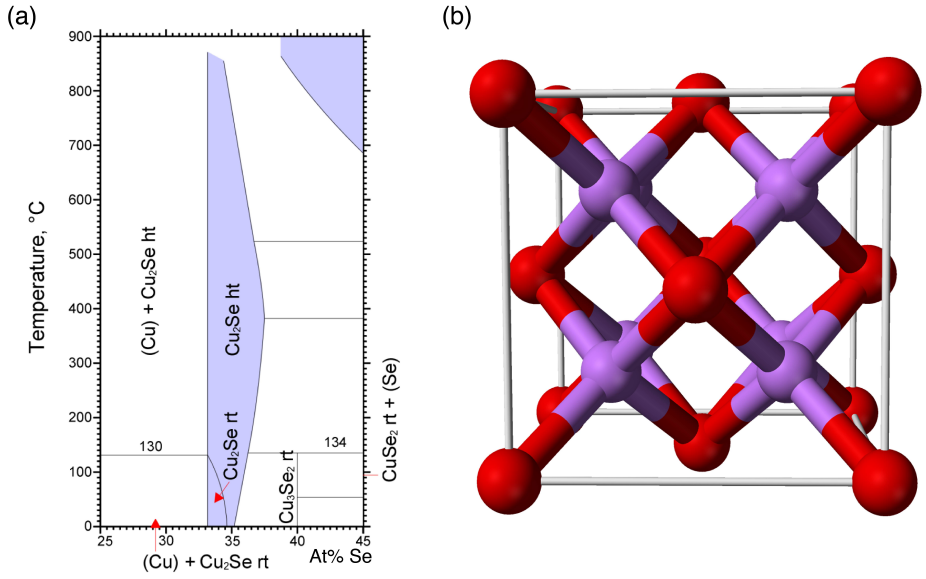

Figure 5.8: Phase diagram (a) of Cu-Se system in the vicinity of Cu_2Se adapted from Heyding [78]. The phase transition is between the $\beta - Cu_2Se$(RT) phase and the $\alpha - Cu_2Se$(ht) phase. Anti-fluorite structure (b) of which $\alpha - Cu_2Se$ is a modification. Se is coordinated FCC and is represented in red. Ground state Cu is tetrahedral coordinated to the Se though significant occupation of trigonal planar and octahedral interstitials has been measured. The structure of $\beta - Cu_2Se$ is unknown.

drawing intercepting tangents to the behavior before and during the rise, the phase transition temperature is determined to be approximately 407 K. This agrees with the temperature of 408 K determined above by crystallography.

Both crystallographic and calorimetric studies indicate Ag_2Se to have a phase transition at $408K$.

5.3 Cu_2Se

The description of the phase transition behavior of Cu_2Se is complicated by the unsettled argument over the nature of that phase transition and the structure of the low temperature phase. The high temperature phase is at this point fairly well understood. The material is a known, if not abundant, mineral under the name of Berzelianite. During the same work in which he indexed high temperature Ag_2Se, Rahlfs also indexed high temperature $Cu_{1.85}Se$ [161]. All the compositions of $Cu_{2-\delta}Se$

from $\delta = 0$ to $\delta = 0.2$ appear to have the same high temperature anti-fluorite cubic structure [78, 194, 201]. (Figure 5.8) Though that phase is on average anti-fluorite, significant Cu^+ occupation of trigonal planar and octahedral interstices is observed [201]. Hopping through these interstices is the mechanism of fast copper ion transport; the ion transport pathways have been successfully determined to be along the [111] direction from tetrahedral to trigonal planar intersticies [43, 42].

Despite Cu_2Se presence in mineral form and its binary compositon, the ordered low temperature structure is yet unknown. This is not for lack of trying. In 1987 Milat *et al.* [134] proposed a monoclinic supercell and in the course of that work noted eleven other proposed structures. They proposed a structure that assumed significant octahedral occupation. Later authors proposed more complex superstructures [123, 96]. These structures are insufficiently complex to explain the crystallography data presented below.

Multiple authors have proposed a co-existence transformation between the α and β phase with a temperature width of 10's of Kelvins [41, 188, 121]. This hypothesis, though reasonable, is contradicted by the data presented in this chapter. There are three reasons for this. The $Cu_{1.8}Se$ is commensurate with the α Cu_2Se. In the region $\delta = .05$ to $\delta = .2$ there actually is a coexistence of the β-Cu_2Se phase and the $Cu_{1.8}Se$; if the phase diagram is determined imprecisely, the single phase region goes unnoticed. Finally, unknown errors in synthesis have led to samples showing impurity phases of $Cu_{1.8}Se$ [121]. As room temperature $Cu_{1.8}Se$ has the same structure as $\alpha - Cu_2Se$ [78], this is an easy confusion to make. There is indeed co-existence of $\beta - Cu_2Se$ and $\alpha - Cu_{1.8}Se$ in such samples, but it is a co-existence of admixture rather than that of synthesis. Vengalis *et al.* [190] observed that this phase tends to form on the grain boundaries of copper rich phases.

Prior to this work the 410 K phase transition was believed to be first order. This is unsurprising, as it takes careful measurement and analysis to differentiate a lambda second order transition from a first order transition. The difficulties of this determination are well illustrated in the case of the lambda transition of β quartz [184, 82]. As late as 1980 authors were still confused about the lambda nature of its

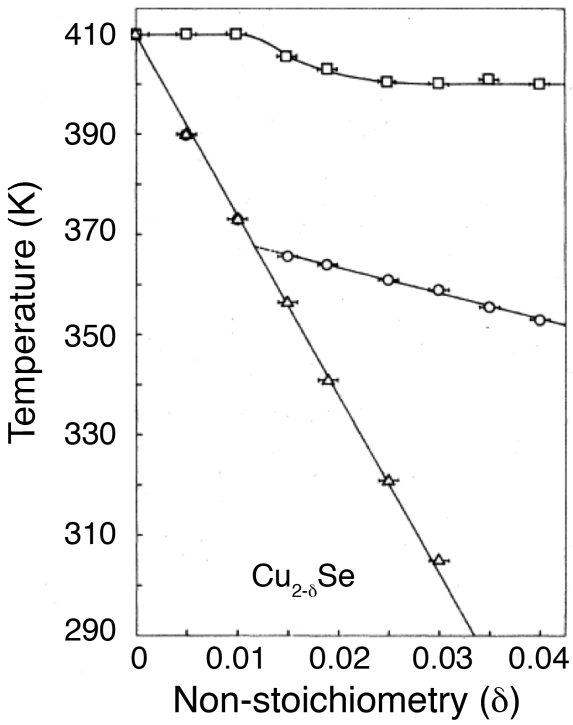

Figure 5.9: The phase diagram of Cu_2Se in its single phase region by Vucic.[194] This diagram was established by dilatometry. Notably, there are multiple phase transitions.

phase transition [82]. While structural second order transitions with diverging heat capacity are of interest to the physics community, they are far less common than first order transitions. Korzhuev determined Cu_2Se's transition to be first order on the basis of the Clausius-Clapeyron relations [105]. However, Pippard showed than an analagous relation holds for lambda-type transitions [157]. Vucic determined it to be first order on the basis of its sharp feature in their dilatometry data [191]; again, such sharp features are also expected in the case of a lambda-type second order transition [157]. Qualitative assesment of sharpness of thermophysical peak at a phase transition temperature can differentiate a first order transition from a second order transition without diverging heat capacity [140]; it is insufficient for differentiating a first order transition from a lambda-type second order transition.

Despite this confusion there is some certainty about the phase diagram at room temperature. By electrochemical determination [197] Korzhuev *et al.* found there to be a single phase region of $Cu_{2-\delta}Se$ [101] for $\delta = 0$ to $\delta = 0.05$ and a range of co-

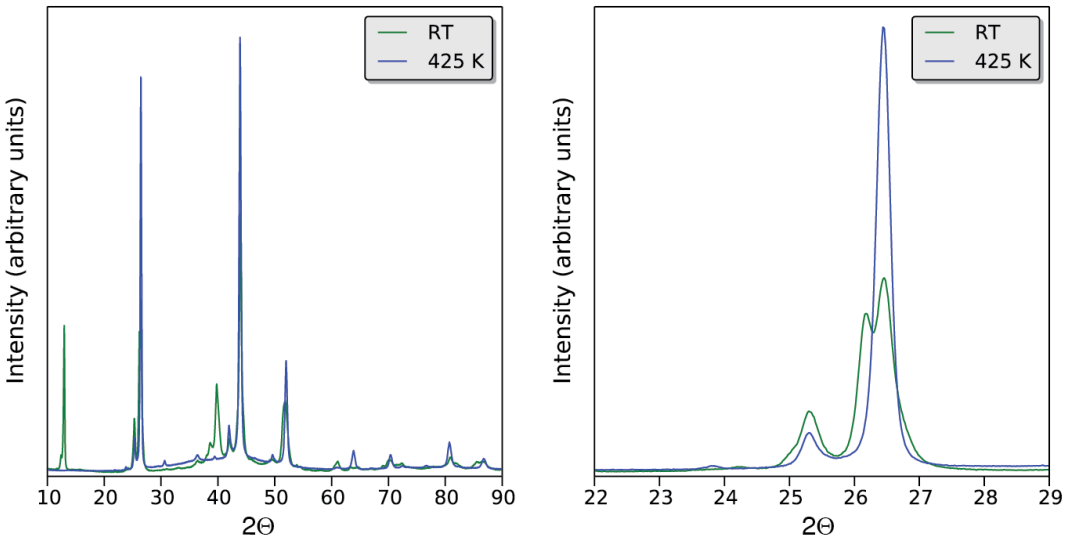

Figure 5.10: Left:PXRD of Cu_2Se at 300 K and 425 K from $2\theta = 10°$ to 90°. Right: Zoom in near the 26° peak set. Peaks positions as identified in literature were observed [96]. The sample is single phase.

existence of $Cu_{1.95}Se$ and $Cu_{1.8}Se$ from $\delta = 0.05$ to $\delta = 0.20$. Temperature dependent dilatometry was performed by Vucic *et al.* in the single-phase region, and he developed a phase diagram on this basis, see Figure 5.9. Vucic's collaboration made follow up transport measurements [194, 134, 84, 192]. In general our sample shows the properties that Vucic observed in his samples of nominal composition $Cu_{1.99}Se$.

5.3.1 Diffractometry

A diffractogram was measured at room temperature from $2\theta = 10°$ to $2\theta = 90°$. The sample was then heated at 1 K per minute to 425 K (above the nominal phase transition temperature of 410 K. A second diffractogram was taken at 425 K. These diffractograms are shown in Figure 5.10. The low temperature diffractogram is consistent with literature reports [96]. The bifurcation of the major $\alpha - Cu_2Se$ peaks in the $\beta - Cu_2Se$ phase is consistent with the β phase being a monoclinic or orthrhombic modification of the anti-fluorites structure. $Cu_{1.8}Se$ impurity phase observed by Liu et al. was not observed here [121].

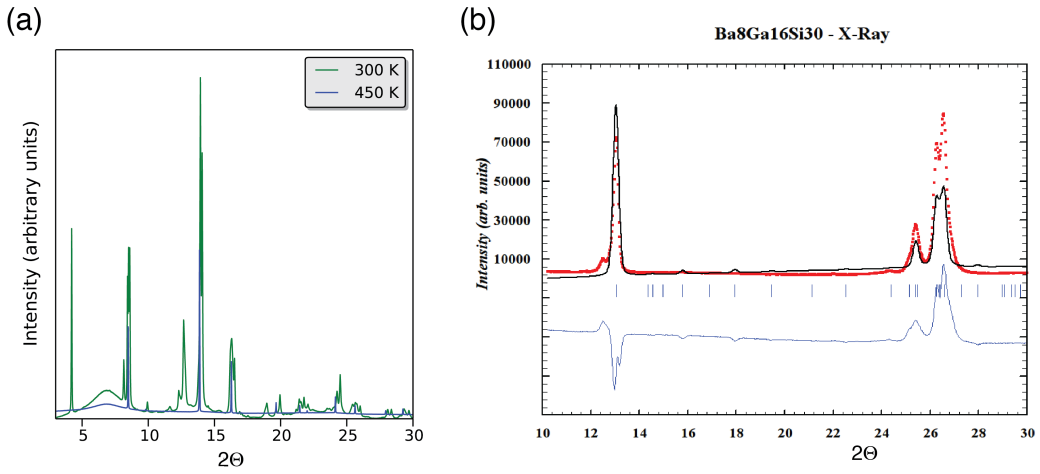

Figure 5.11: High flux low angle synchotron data of Cu_2Se (a) shows significant strong reflections, indicating that a large unit cell to explain the data. The recent models of Liu *et al.* [123] show a better fit than those previously published, [134, 96] but cannot explain all the low angles peaks observed (b). In (b) the black line is the data, the red line the model, and the blue line their discrepancy. Courtesy of Kasper Borup.

My crystallography collaborators were unable to resolve the low temperature structure. They determined that though many authors have proposed structures for Cu_2Se, these structures use a large enough unit cell to explain all of our observed peaks and their intensities. Many of these proposed structures are based on analysis of lower signal to noise diffraction data than that presented here; consequently, those authors propose structures that are too simple. Kashida and Akai [96] proposed a monoclinic unit cell ($a = c = 7.14\,\text{Å}$, $b = 81.9\,\text{Å}$, $\beta = 120°$) with ordering of copper vacancies, while Milat et al. proposed an even larger monoclinic cell ($a = c = 12.30\,\text{Å}$, $b = 40.74\,\text{Å}$, $\beta = 120 \pm 1°$). [134] Neither of these unit cells were able to describe the position of all reflections at low angles observed via high flux synchrotron.(Figure 5.11(a)). This indicates the structure to be even more complicated. These low angle peaks were not measured previously with the precision done in this experiment. Since publication of my paper [23], Liu *et al.* [123] proposed a triclinic unit cell ($a = 7.12\,\text{Å}$, $b = 7.14\,\text{Å}$, $c = 7.51\,\text{Å}$, $\alpha = 98.6°$, $\beta = 107.6°$, $\gamma = 60.1°$) and a monoclinic unit cell ($a = 7.13\,\text{Å}$, $b = 12.36\,\text{Å}$, $c = 14.47\,\text{Å}$, $\beta = 100.4°$) with larger unit cells than that proposed before. These structures were also unable to clar-

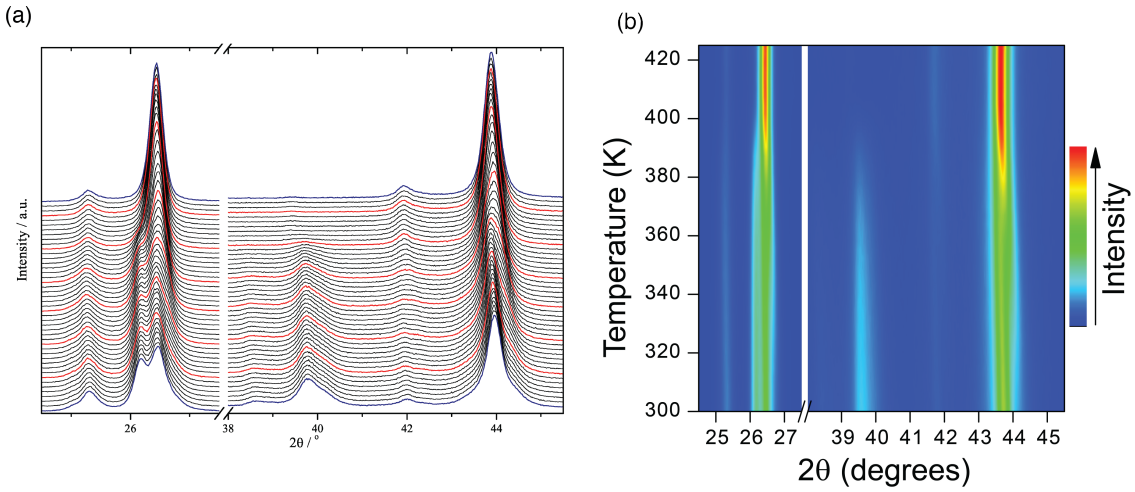

Figure 5.12: Temperature varied diffractograms of Cu_2Se. Data is presented as stacked diffractograms (a) and as a color map (b). The peak intensities and angles shift continuously from the low temperature to the high temperature phase.

ify all of our observed peaks nor determine their intensities correctly. This is shown for the proposed monoclinic structure in Figure 5.11(b). Therefore, no structural refinement below the phase transition is possible from PXRD at present, and the order parameter is not easily obtained from this method.

The 425 K diffractogram (Figure 5.10) is well fit by an anti-fluorite structure with the exception of a few anomalous peaks. These anomalous peaks are not present in the synchotron data from 450 K, see Figure 5.11, suggesting that either the phase transition is not fully complete at 425 K or that insufficient time was taken to let the kinetics stabilize at 425 K before measuring the diffractogram. Based on the PXRD and synchrotron data I conclude that the Cu_2Se measured for this study is single phase and in concordance with other single phase samples synthesized for literature studies.

For crystallographic determination of the nature of the phase transition, diffractometry must be performed at a series of temperatures that transverse that transition. During the heating process to 425 K for obtainment of the diffractogram of $\alpha - Cu2Se$ (Figure 5.10), diffractograms were continuously measured from $2\theta = 23°$ to $2\theta = 45°$. The duration of each scan was three minutes and consequently the temperature changed by 3 K from start to end of each scan. The 2θ range was chosen

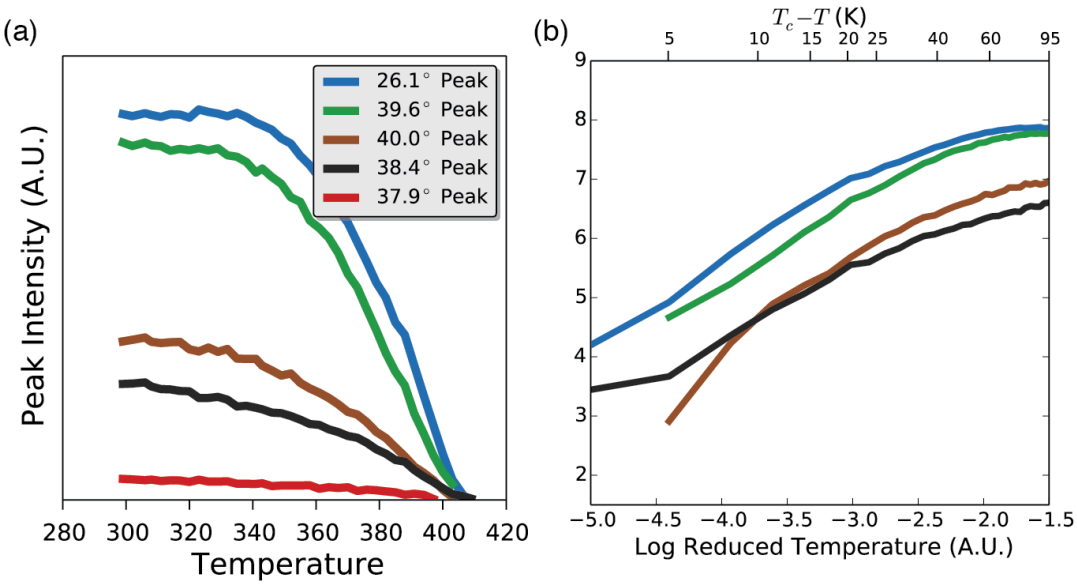

Figure 5.13: Peak intensities versus temperature (a) for selected peaks of Cu_2Se. These peaks were chosen because they only appear in the low temperature phase. They show a continuous decrease to the phase transition temperature. This decrease corresponds well with a critical power law, as seen by the linearity of log-intensity versus log-reduced temperature.

because of the excellent signal intensity and the two separate bifurcated peaks seen. Visualization of this data (Figure 5.12) shows a continuous evolution of the bifurcated peaks at low temperature into the single peaks at high temperature. Both the peak intensities and angles shift continuously from the low temperature to the high temperature phase. This strongly contrasts with the abrupt change that would be seen as in a first order transition (*i.e.*, that of Ag_2Se presented above in Figure 5.6). Cu_2Se does not have a first order transition.

Detailed analysis of the temperature resolved PXRD data confirms Cu_2Se's phase transformation to be continuous. For a second order phase transition, it is expected that a crystallographic order parameter should go to zero with some exponent of the reduced temperature $\tau_r = (T_c - T)/T_c$. To examine this effect, we plot the peaks that disappear at the phase transition temperature (Figure 5.13(a)). These peaks show critical power law behavior as the phase transition temperature is appraoched (Figure 5.13(b)). The data at the phase transition is insufficiently detailed to ex-

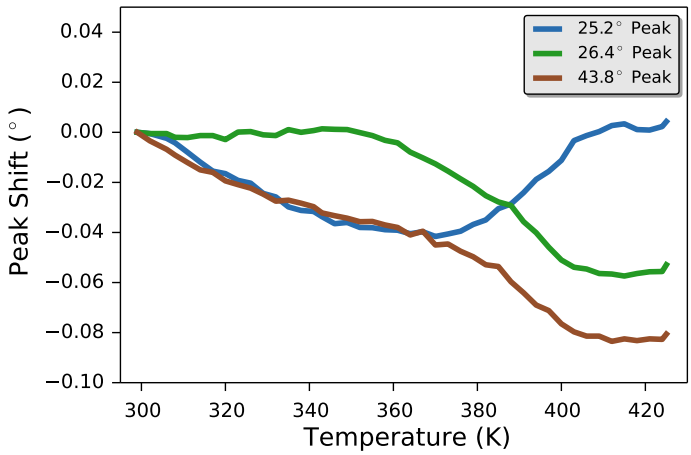

Figure 5.14: Temperature dependence of the peak shift for representative diffraction peaks of Cu_2Se. The peak shifts are incompatible with a coexistence transformation.

tract a precise critical exponent; the data resolution for such a fit must be increase exponentially higher as the phase transition temperature is approached. The critical exponents so obtained would be far larger than unity. This is greater than the critical exponent expected for the Ising model [95] and found in other super-ionic transitions [118]. It is therefore likely that while the critical exponents of the peaks are related to the order parameter, their critical exponent is not that of the order parameter (canonically labeled β). T_c was determined to be 408 K, as that temperature gave approximately the some slope in Figure 5.13(b) for angles analyzed. This critical temperature is consistent with that found in the literature and determined by other thermophysical measurements for this thesis. The noise floor near the phase transition temperature prevented analysis of the critical exponent for the $2\Theta = 37.9°$ peak.

The shift in peak angles with temperature is inconsistent with an $\alpha \rightarrow \alpha + \beta \rightarrow \beta$ coexistence transformation. In a coexistence transformation the secondary peak in the bifurcation should be stable in peak position as its intensity increases, varying only due to thermal expansion. In contrast a second order transition the peaks will bifurcate smoothly from one another. The peak positions of Cu_2Se show such shifts in the temperature range from 360 K to 410 K. (Figure 5.14) Notably the $2\Theta = 25.2°$

and 26.4° shift in opposite directions; this is inconsistent with thermal expansion.

The phase diagram of Vucic (Figure 5.9) anticipates a (non-lambda) second order transition at a lower temperature. At 360 K there is a point of inflection in the peak shift of the $2\Theta = 25.2°$ and 26.4° peaks. The peak intensity and shifts in general begin to shift significantly at this temperature. While that is not definitive evidence of a second order transition at 360 K, more data relevant to that point will be presented later in this document.

A pair distribution function (p.d.f.) was obtained from total scattering data. It describes the distribution of distances between pairs of atoms in the structure. The changes of the p.d.f. are gradual, indicating that the ordering of Cu-interstitials occurs over a wide temperature range. There is no evidence of a first order discontinuity in peak positions nor of the β phase being present below 410 K. The phase transition does not appear to be complete until 450 K; transformation above the phase transition temperature is characteristic of second order transitions. The $Q_{max} = 26$Å used is insufficient for truly accurate quantitative fitting, as indicated by the presence of substantial integration error ripples below the first peak maxima.

Even without modeling the data it is possible to extract qualitative information. By studying the high-temperature structure of Cu_2Se it is clear that the peak at 4.1 Å (Figure 5.15(a)) is a superposition of the shortest Cu-Cu and Se-Se distances in the [110]-direction. Above 300 K the peak becomes increasingly asymmetric, indicative of multiple Cu-Cu distances in the high-temperature phase related to the disorder of Cu interstitials. At low temperature the Cu order to form a superstructure. The superstructure formation is most clearly seen in the region 8 Å to 9.5 Å (Figure 5.15(b)). This range corresponds to Cu-Cu distances in the [110]-direction in adjacent cubic unit cells. Below 410 K there are two distinct peaks at 8.2 Å and 9.3 Å. However in the high temperature phase the same region is a continuum of overlapping peaks arising from the disorder of Cu.

Theoretical models of super-ionic conductivity assume that it is due to Frenkel defect formation — that a number of interstitial sites similar to the number of ions become occupiable in the higher temperature phase [21, 163, 70]. Such significant

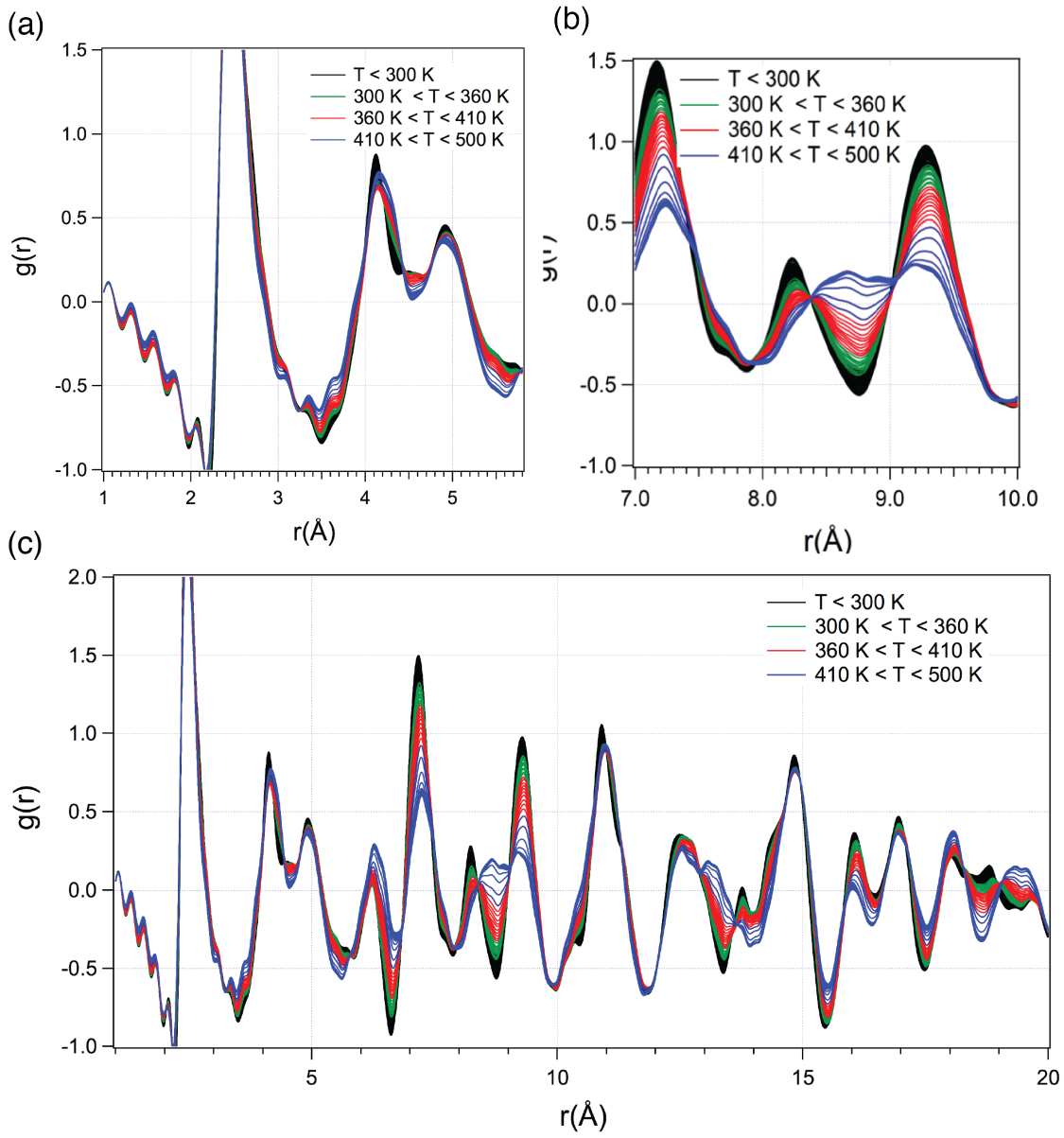

Figure 5.15: Pair distribution function data for Cu_2Se. The unit cell size is 5.8 Å. The coordination number remains the same through the phase transition (a) but correlations between high temperature equivalent unit cells breaks down.(b) Full data set. (c)

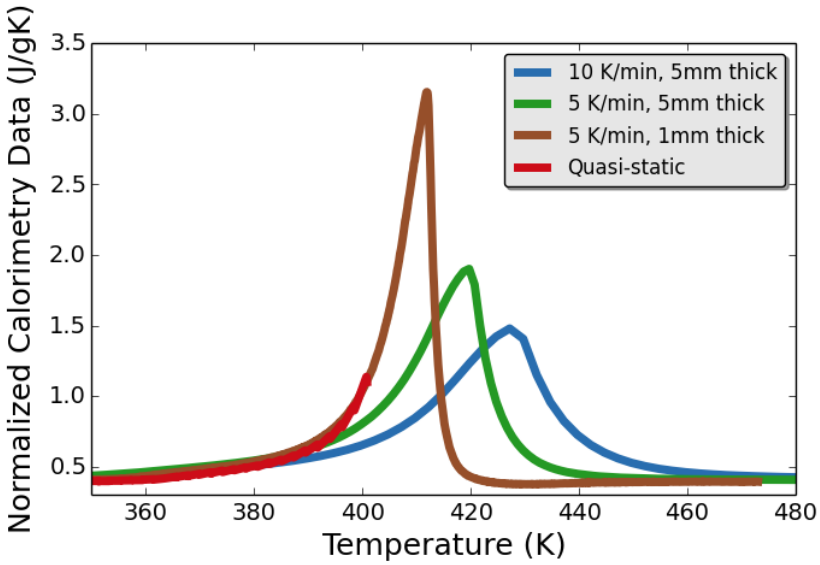

Figure 5.16: Calorimetry data for Cu_2Se under differing measurement condition. As the diffusive time scale is decreased, the data converges to the quasi-static heat capacity measured by Quantum Design Physical Property Measurements System (PPMS). The phase transition temperature is marked with a black dotted line. Data courtesy of SIC-CAS and the JPL Thermoelectrics Group.

Frenkel defect formation should result in new peaks in $g(r)$ for r less than the lattice spacing of the high temperature phase ($5.8\mathring{A}$). While the peaks in this range are broadened, Figure 5.15(a), there is nothing to suggest significant new site occupation. For unit cells greater than 5.8 Å a much more substantial change is observed. (Figure 5.15(b)) This suggests that the correlations between high temperature unit cells breaks down substantially. The implication of this is that rather than the disordering being due to Frenkel defect formation, it is primarily due to a breakdown of correlations between unit cells, as represented by the 8.2 Å and 9.3 Å peaks. It is unclear at this time what the microscopic mechanism for correlations between unit cells is. One possibility is that the order state of the super-ionic transition is supported by a local electronic polarization like in a ferroelectric.

5.3.2 Cu_2Se Calorimetry

Calorimetry data also supports Cu_2Se being a second order transition. In order for a DSC measurement to accurately represent a material's heat capacity, the heating rate should be much faster than the timescale of thermal equilibriation. At a first order transition there is an instantaneous enthalpy release. This enthalpy cannot be transported out of the material instantaneously, and so a temporary difference between the temperature of the bath and the temperature of the sample occurs. Therefore, a first order phase transition will show a peak of finite width at its phase transition. For example, in the Ag_2Se calorimetry curve presented above.(Figure 5.7(a)), the heat capacity is elevated over the Dulong-Petit baseline from $405K$ to $420K$. Over this temperature range the sample is not in thermodynamic equilibrium with the bath. For the phase transformation to be complete a quantity of heat equal to the enthalpy of formation may be added, but the rate at which heat may be added is limited by the material's thermal diffusion time scale (t_D) and its heating rate ($\dot{T}$). This can be written mathematically as:

$$\delta T = A t_D \dot{T}, \tag{5.7}$$

in which A is a constant term that serves as a catch-all for the geometric configuration of the apparatus and sample. As discussed in Chapter 2 in the context of thermal diffusvity measurements, the diffusion time scale is related to the diffusion length (l_D) by $t_D = l_D \cdot D_t^{-1}$. This provides a scaling relation by which measurements on different size samples and heating rates can be compared.

$$\delta T = A \frac{l_D^2}{D_T} \dot{T} \tag{5.8}$$

Because of the smearing of the enthalpy of formation, it is easy to accidentally mistake a second order transition with diverging heat capacity for a first order transition. The historical case of the β-quartz transition exemplifies this difficulty [85]. Considerations based on heating rate and sample size have proved successful in the past for differentiating first and second order phase transitions [140].

The enthalpy released per unit temperature of a lambda-type transition is always finite. However, the low thermal diffusivity and non-linearity in the heat capacity may still lead to errors in the DSC derived heat capacity. A fixed temperature rate induces an error in the heat capacity resolution due to the sample's thermal diffusivity. Two separate samples were sent to SIC-CAS and JPL for DSC measurement. The heat capacity measured at these two facilities showed markedly different calorimetry curves (Figure 5.16) that can be explained by Equation 5.7. The JPL sample had a thickness of 2.5 mm, while the SIC-CAS sample had dimensions of approximately 0.8 mm. On this basis the 5 Kelvin per minute and 10 Kelvin per minute JPL measurements are expected to have a temeprature errors 10 and 20 times that of the SIC-CAS sample. The maximum of three curves are at 412 K, 420 K, and 427 K, which corresponds well to the predicted trend and indicates an error on the SIC-CAS temperature resolution of less than 1 Kelvin.

On this basis the c_p derived from the SIC-CAS DSC measurement is judged to be accurate enough for calculating transport data. The DSC heat capacity was further confirmed via the quasi-static method of the Quantum Design Physical Property Measurement System to 400 K with the assistance of Dr. Xun Shi of SIC-CAS. In this methodology the temperature is stabilized before the heat capacity is measured. Within each three point set the variation in measured heat capacity is less than 1%, indicating that the equilibrium condition was met. These measurements confirm that the heat capacity is increased at the phase transition temperature.

At 355 K there is a distinct change in the slope of the heat capacity.(Figure 5.17) This is consistent with a (non-lambda) second order phase transition and the predictions of Vucic. This extended elevation is inconsistent with a first order transition and consistent with a second order transition. There is a distinct change in the slope of c_p with T at 355 K. That feature is indicative of another second order phase transition and accords with the phase diagram of Vucic. A feature near this temperature was observed in the temperature crystallographic measurements discussed in the previous subsection. The calorimetry data is consistent with two second order phase transitions at 360 K and 410 K. The transition at 360 K has a heat capacity that converges

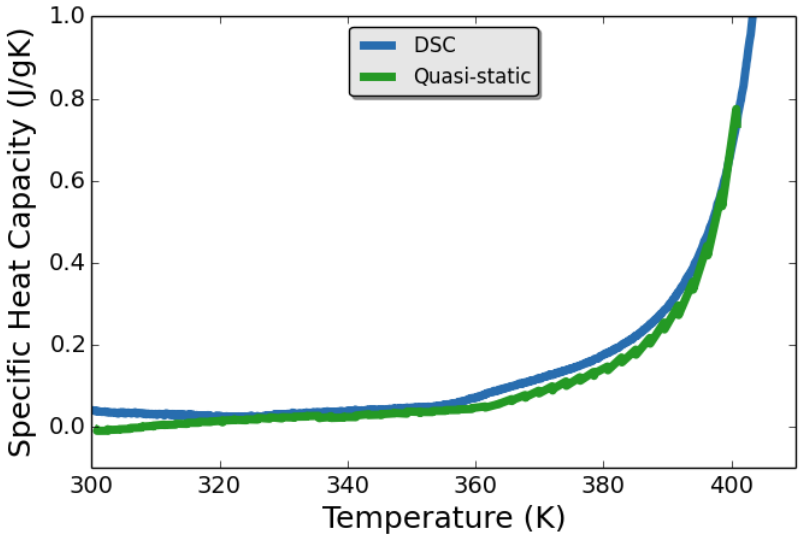

Figure 5.17: Heat capacity minus Dulong-Petit heat capacity below the phase transition temperature. Data is shown both for the DSC measurement and the quas-static PPMS measurement. The non-linear elevation in heat capacity begins at $355K$.

to zero, while the transition at 410 K has a divergent heat capacity.

5.4 $Cu_{1.97}Ag_{0.03}Se$

At room temperature the material's main phase has a structure related to the room temperature structure of Cu_2Se. This structure has not been satisfactorily solved in the literature but it is believed to be equivalent to the high temperature structure but with ordered Cu vacancies and interstitials. The ordering is believed to depend highly on the exact stoichiometry, which may explain the lack of a unit cell that describes the low temperature structure. Of the peaks that could not be related to Cu_2Se peaks, CuAgSe and at least two distinct impurity phases are identified. At least one impurity phase is still present at high temperature and at least one impurity phase dissolves at the phase transition at 400 K, see Figure 5.18. The CuAgSe impurity phase is clearly visible in scanning electron micrographs of the sample, see Figure 5.19. The impurity peaks that dissolve do not have corresponding peaks in Cu_2Se and are hence believed to be impurities; however, it is possible that they belong to the main phase if this has

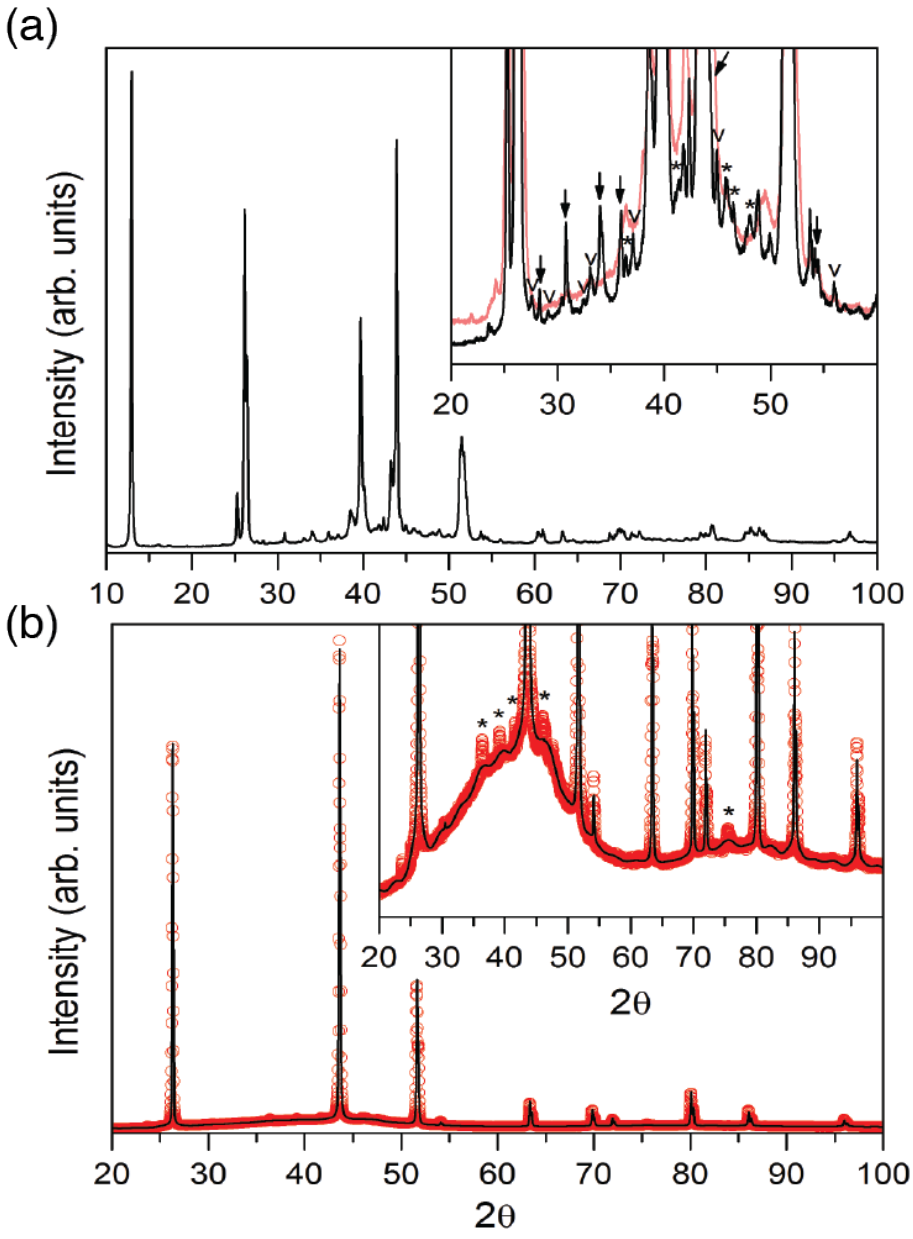

Figure 5.18: Room temperature (a) and 450 K (b) diffractograms of $Cu_{1.97}Ag_{0.03}Se$. Impurity peaks marked v disappear at the phase transition, while those marked * remain. Peaks marked with an arrow correspond to CuAgSe. Courtesy of Kasper Borup.

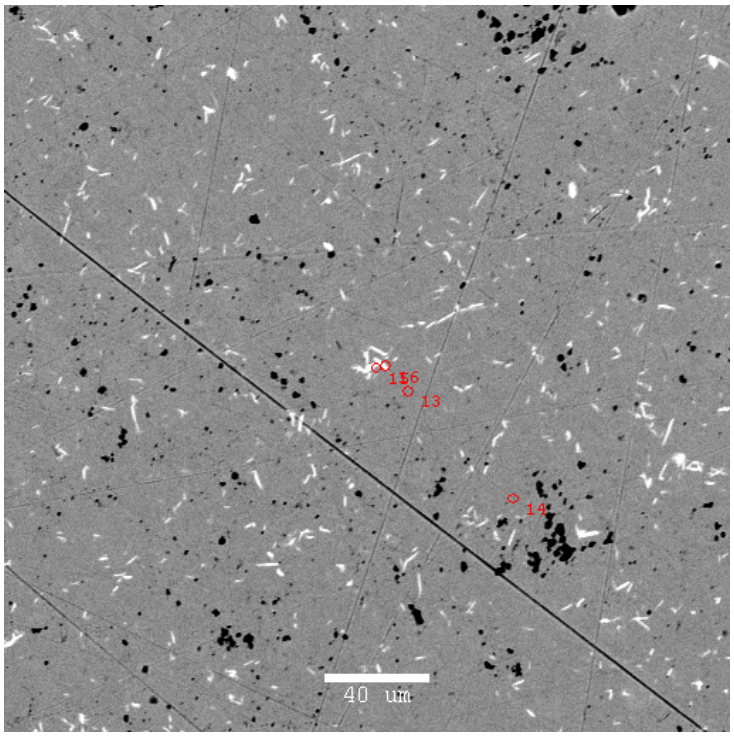

Figure 5.19: Scanning electron micrograph of $Cu_{1.97}Ag_{0.03}Se$ courtesy of Tristan Day. Gray areas are Cu_2Se phase, black areas are voids and white areas are CuAgSe

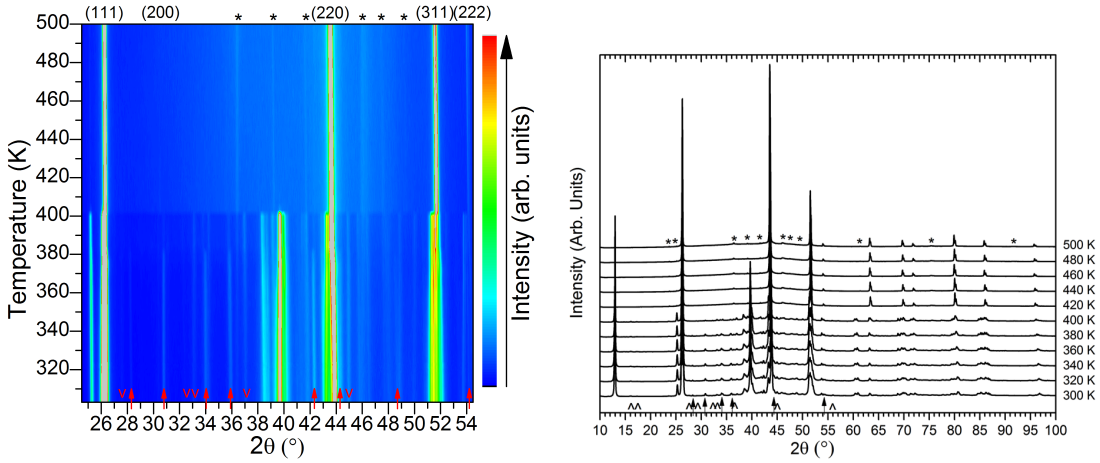

Figure 5.20: Left: Color map of temperature varied diffactrograms of $Cu_{1.97}Ag_{0.03}Se$. Right: Slower diffractograms were performed at 20 K intervals. Impurity peaks marked v disappear at the phase transition, while those marked * remain. Peaks marked with an arrow correspond to CuAgSe and dissolve at 380 K. The high temperature reflections of Cu_2Se are labeled on top of the graph. Courtesy of Kasper Borup.

a structure different from Cu_2Se.

Diffractograms were measured on constant heating continuously from $2\theta = 24°$ to $2\theta = 55°$. A color map is presented in Figure 5.20(a). The duration of each scan was three minutes and consequently the temperature changes by 3 K from start to end of each scan. During heating, dissolution of CuAgSe was observed at 380 K. At ≈400 K there was a structural transition of the primary phase to a high temperature structure, which remained present and unchanged to 500 K. All peaks except few low intensity impurity peaks (also present at room temperature) can be indexed and refined with the high temperature Cu_2Se structure. Every 20 K higher quality diffractograms were recorded, during which the sample was held at constant temperature for at least 45 minutes. At 380 K, CuAgSe was present and unchanged both before and after the 45 minute scan, and hence this is not believed to affect the dissolution. No change in CuAgSe is observed until the diffractogram labeled 384 K (scans are labeled according to the sample temperature when they are started). The same is true for the primary phase and dissolved impurity at 400 K.

The structural phase transition has both a first and second order component. The

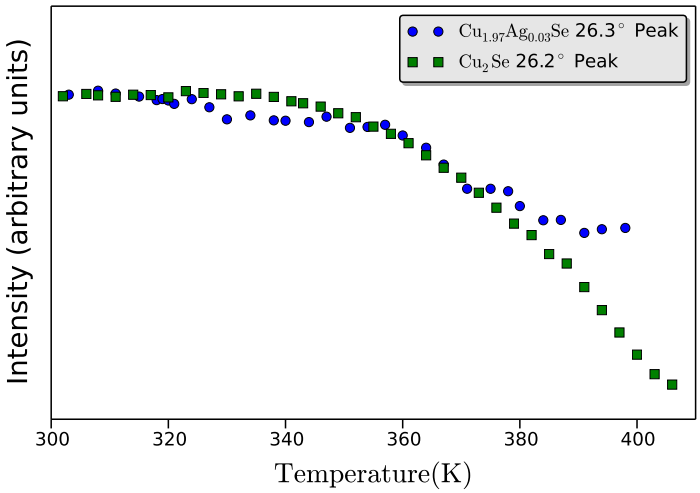

Figure 5.21: Comparison of the $2\Theta = 26.2°$ peaks of both Cu_2Se and $Cu_{1.97}Ag_{0.03}Se$. All units are arbitrary and scaled to be identical at $T = 300\,K$. Up to 380 K the peak of $Cu_{1.97}Ag_{0.03}Se$ follows the second order trend of Cu_2Se. On dissolution of CuAgSe at 380 K its intensity stabilizes while temperature increases, until the first order transition at $\approx 400\,K$ eliminates the peak entirely.

structure is gradually changing from room temperature and up. This is evidenced by the peaks moving relative to each other while the intensities also change. At the dissolution of CuAgSe there is a strong change, and again this appears not to be due to the 45 minute rest at 380 K. The dissolution of CuAgSe seems to result in a faster rate of transition. Contrary to pure Cu_2Se, many peaks seem to be shifting position, while others seem to only change intensity (except for a slight shift due to thermal expansion).

5.4.1 Cu_2Se and $Cu_{1.97}Ag_{0.03}Se$

From the crystallography data $Cu_{1.97}Ag_{0.03}Se$ appears to have an *interrupted* and distorted version of the second order transition of Cu_2Se, *i.e.*, it appears to be a weakly first order transition .The distortion occurs on dissolution of the secondary CuAgSe phase near 380 K. The interruption occurs at 403 K at which point the transition becomes first order. This behavior is best seen by comparing the temperature dependence of peak intensity of the $2\Theta = 26.2°$ peaks of both Cu_2Se and $Cu_{1.97}Ag_{0.03}Se$.

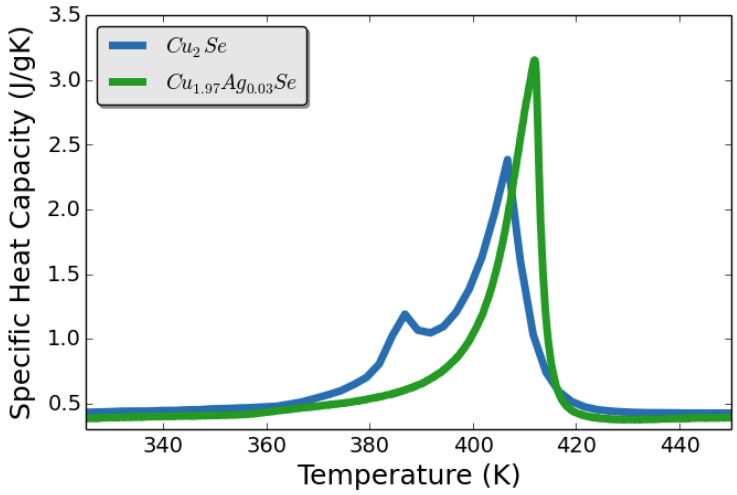

Figure 5.22: Differential scanning calorimetry for $Cu_{1.97}Ag_{0.03}Se$ in comparison with that of Cu_2Se.

Up to 380 K the peak of $Cu_{1.97}Ag_{0.03}Se$ follows the second order trend of Cu_2Se. On dissolution of CuAgSe at 380 K its intensity stabilizes while temperature increases, until the first order transition at $\approx 400\,\mathrm{K}$ eliminates the peak entirely. These trends strongly affect the temperature dependence of $Cu_{1.97}Ag_{0.03}Se$'s transport behavior, as is to be discussed later in this thesis.

The heat capacity of $Cu_{1.97}Ag_{0.03}Se$ shows a doubled peak, see Figure 5.22 The temperature of the first peak corresponds to the temperature dissolution of the CuAgSe phase observed by crystallography. The temperature of the second peak corresponds to the first order transition. Some of what is labeled as specific heat in Figure 5.22 is surely enthalpy of formation due to the first order component of the phase transition. However, at this time I am unable to distinguish which portion belongs to the second order transition and which to the fist order transition. I will treat all the measured enthalpy from the DSC measurement as if it were due to a second order transition. This will lead to an overestimate in c_p and therefore an underestimate of zT, but I feel it is best to be conservative in my calculation.